

**OPTIMIZATION OF THERMAL SPRAY PARAMETERS FOR
CATHODIC PROTECTION OF REINFORCEMENT IN CONCRETE**

C.C. Berndt and S. Reddy
State University of New York at Stony Brook
The Thermal Spray Laboratory
Stony Brook, NY 11794-2275

M. L. Allan
Brookhaven National Laboratory
Department of Applied Science, Building 526
Upton, NY 11973

ABSTRACT

Thermal spraying of zinc as an anode material is an effective means of providing **cathodic** protection to reinforced concrete. An empirical modeling technique **was** used to optimize the properties of the zinc coating and make the thermal spray parameterization efficient. The two properties optimized in this study were tensile adhesion strength of the coating, **which** gives a measure of durability; and deposition **efficiency**, which is a measure of the process efficiency and, therefore, the process **economics**.

A novel single wire arc plasma system was used to apply the zinc coatings. The parameters varied were (i) torch to substrate distance, (ii) cooling gas pressure and (iii) arc current. The results of the modeling indicate that the torch to substrate distance and gas pressure exert greater control over tensile adhesion strength and deposition efficiency than arc current.

Keywords: thermal spray process, process parameterization, zinc coatings, adhesion strength, **cathodic protection**, concrete.

INTRODUCTION

Thermal Spraying and Cathodic Protection

Successful cathodic protection of steel reinforcement in concrete using thermal sprayed zinc anodes has been **demonstrated**.¹⁻⁴ Zinc coatings offer an alternative to anodes such as titanium mesh and conductive polymer wire **which** require an overlay. Advantages of thermal sprayed zinc coatings include ability to cover complex surfaces, uniform current distribution and redundancy of an overlay. Another potential advantage is use of the zinc coating as a **sacrificial** anode in conditions of low concrete resistivity as opposed to an impressed current anode.

Cathodic protection systems formed by the thermal spray process may require tons of zinc for a single structure and the coating is required to provide several decades of service. Therefore, the deposition process **must** be optimized so that

Publication Right

Copyright by NACE International. NACE International has been given first rights of publication of this manuscript. Requests for permission to publish this manuscript in any form, in part or in whole must be made in writing to NACE International, Publications Division, P.O. Box 218340 Houston, Texas 77218-8340. The material presented and the views expressed in this paper are solely those of the author(s) and are not necessarily endorsed by the Association. Printed in the U.S.A.

material consumption is minimized and so that the coating adheres to the concrete and provides adequate cathodic protection to embedded reinforcement throughout the service life. Factors **affecting** adhesion of thermal sprayed zinc onto concrete such as surface temperature, surface preparation technique and concrete moisture content have been **reported**.^{5,6} In the study presented here, optimization of thermal spraying parameters is investigated with the aim of **identifying** the aspects of the application process which are critical to coating adhesion and deposition efficiency (DE).

Thermal spraying of zinc wire using a new process, the Single Wire Arc Plasma (SWAP)⁷ system was performed. The DE (*i.e.*, ratio of the amount of material deposited to the amount sprayed) and the adhesion strength to concrete were maximized using an optimization process called Response Surface Methodology (**RSM**).^{8,9}

Thermal Spray Processes

There are many possible methods to thermal spray zinc onto concrete; for instance, oxy-acetylene wire flame spraying, two wire arc spray and single wire arc-plasma spraying. The coating properties and process economics depend on the thermal spray method employed. A demonstration **study** commenced in 1983 used the oxy-acetylene process to spray the **Richmond-San Rafael Bridge** in **California**¹; however the current trend is towards arc spraying.

In the current work, the SWAP process was chosen since it was of novel character and was claimed to have certain attributes over other thermal spray systems. The SWAP system had not been **studied** for applying thermal sprayed zinc for cathodic protection. The process uses a **non-consumable hafnium/copper** cathode and a consumable anode wire (*e.g.*, zinc), Fig. 1.⁷ An arc is struck between the cathode and anode. The energy of the arc is used to initiate the plasma which is maintained by ionizing the primary plasma **gas** (*i.e.*, air) and applying a potential between the wire and the cathode. The plasma gases flow around the cathode and toward the melting wire anode. The primary plasma gas performs two functions; it cools the cathode and it is **used** to initially atomize the molten droplets. A secondary gas flow (air) is also used to further atomize the molten droplets and propel them towards the substrate.

Process Optimization and Parameterization

Thermal spraying requires equipment and process adjustments (termed as "spray parameters") which are based on equipment **manufacturer's** recommendation **and/or** the experience of a **thermal** spray applicator. To optimize a thermal spray process it is necessary to understand the relationship between properties and spray parameters and this can be performed by empirical **modeling**.⁸ In this study the following definitions are used. A **process** is the method which is used to manufacture a zinc coating. A **property** is normally defined as the characteristic of the material that is important to an engineering application; in this study tensile adhesion strength is the property being optimized. Deposition efficiency, even though it is not a characteristic of a material, but a characteristic of the process conditions, will also be considered as a property. A **parameter** is defined as a setting or variable that the operator can change to **affect** the property. Examples of parameters used in arc plasma spraying are **primary** gas flow, secondary gas flow, standoff distance, and arc current. The term **substrate** is used to **identify** the concrete specimens that were coated.

Empirical models **are** derived from experiment and **observation**.⁹ These models do not provide a physical understanding of how **parameters** influence the property-, *i.e.*, they are not mechanistic models. A recent thrust of thermal spray industry has been the development of more mechanistic models; however, such models **are** quite general and cannot **be** applied to specific **thermal spray** processes because they contain many **approximations** of the physical laws governing the **process**. The procedure of **RSM**^{8,9} is an empirical modeling technique that fits experimental results to a well defined function which is continuous over the region tested. The method relates spray parameters to the coating properties.

The product of a **RSM** test is data representation in the form of either a 3-D plot or a contour plot of spray **parameters** (*i.e.*, gas pressure, arc current and standoff distance) and the coating property (*i.e.*, bond strength and deposition efficiency). The surface detail is limited by the power of each of the parameters used in generating the curve, for example only planar relationships can be shown if an exponent of 1 is used whereas more complex relationships may be revealed by using **higher** powers. However, the use of quadratic polynomials and greater may result in **artifacts** being introduced into the data. Thus, a complex **curve**, having many maxima and **minima**, *can* accommodate large deviations in experimental values caused by errors. A second degree polynomial was used in the present **work** by fitting the data to an equation of the form:

$$Y = b_0 + b_1x + b_2y + b_3xy + b_4x^2 + b_5y^2 \quad \text{Eq.1}$$

where Y = coating **property**; x and y = spray parameters; and $b_0 \dots b_5$ are coefficients determined by **RSM**. Each graph (or surface) requires a minimum of five tests and for the present study nine tests were conducted to increase the confidence level.

An important aspect of applying a **RSM analysis** is to determine the **parameters** that must be optimized. This can be difficult when there are many process parameters which are considered as controlling factors. In the present work three parameters were optimized; **i.e.**, standoff distance (distance **from** the torch to the substrate), arc-plasma current, and secondary gas pressure. These parameters were chosen because they are most likely to be changed by the thermal spray applicator. Preliminary examinations also concluded that these parameters influence **significantly** the properties of the SWAP coating.

Adhesion strength of the coating to the concrete and the deposition efficiency were examined with respect to each process parameter. Response surfaces (3-D) and contour plots (2-D) allowed examination of interrelations between process variables and properties. Curve (or surface) fitting **was** performed using the method of least squares.

EXPERIMENTAL PROCEDURE

Concrete Preparation

Chloride contaminated concrete with a **water/cement** ratio of 0.55 **was** used as the substrate material and the mix was designed to represent that present in older structures, Table 1. Such concrete is most typical of that in need of **cathodic** protection due to chloride induced corrosion of reinforcement. **Superplasticizer**, consisting of a 42% solution of sodium naphthalene **sulfonate** formaldehyde condensate, **was** added to improve workability and to reduce the likelihood of air voids on the cast surfaces. The coarse aggregate **was** 1.2 cm rounded quartz.

Steel molds were used for casting concrete beams with dimensions of 7.6 cm x 10.2 cm x 40.6 cm. Cylinders used for casting compressive strength specimens were 7.6 cm in diameter and 15.2 cm long. The concrete was prepared in a pan mixer and progressively placed in the molds while undergoing vibration on a vibration table. Once cast, the concrete was covered with a wet felt cloth and left to set overnight. The beams and cylinders were demolded after 24 hours and cured in water for 28 days. After curing, the beams designated for adhesion experiments were cut into 10 cm lengths using a cut off **saw**. The **beams** were dried in air for between 2-4 months prior to testing to reduce moisture in the concrete. Some **surface** carbonation may have occurred during this period.

The slump of the concrete was measured according to **ASTM C 143¹⁰** and the average of several batches was 10.9 ± 3.3 cm. Compressive strength at 28 days **was** measured following **ASTM C 39¹¹** and determined to be $42 \text{ MPa} \pm 0.35 \text{ MPa}$.

Spray Coating

The concrete **beams** were used **as** substrates for coating application. These specimens were cleaned by lightly scrubbing the **surface** to remove any contamination and subsequently surface roughened by grit blasting with chilled iron grit at a reduced pressure of 241 kPa rather than the normal operating pressure of 414 kPa. It **was** found that the concrete is severely abraded at the higher pressure and, therefore, the reduction in pressure minimized the exposure of aggregate. It **was** observed that exposed aggregate reduced the bond strength of the zinc coating since the zinc could not adhere well to the relatively smooth surface of the stone. One 10 cm x 10 cm face of these substrates **was** sprayed to a thickness of 0.13 to 0.15 mm for the adhesion tests.

The spray parameters that were varied in this **study** were **gas** pressure, arc current and standoff distance. Three values of each parameter were used, giving a total of 27 **sets** of spraying conditions. Gas pressures were 448, 551 and 690 kPa, arc currents were 30, 45 and 60 A and standoff distances were 5, 10 and 15 cm. Adhesion strength and deposition **efficiency** were measured for the varied parameters.

Deposition efficiency (**DE**) was determined under the same thermal spray parameters used to coat the concrete. The DE is defined as the percent of **material** deposited compared to the amount of material sprayed and can be a deciding factor in the process economics. Grit blasted 15 cm x 15 cm x 0.16 cm steel plate substrates were used to **perform** these tests since such substrates can be considered as infinitely large surfaces and, thus, spray losses due to overspray can be discounted. **The** following procedure **was** used. The wire feeder **was** turned on for 30 seconds and the mass of wire fed measured and a **feed** rate of 1.0 g/sec **was** calculated. Subsequently, the amount of material sprayed **was** calculated by measuring the spraying time. The amount of material deposited is derived by the mass difference of the steel plate before and after spraying; and, therefore the DE **can** be reliably calculated. The use of a steel plate rather than a concrete surface for the DE measurements is not expected to give rise to significant error since the controlling factor in the adhesion of zinc coatings is the **surface** roughness and care **was** taken to ensure that both substrates (steel and concrete) exhibited similar surface characteristics.

Tensile Tests

Tensile adhesion testing of the thermal sprayed zinc coatings on concrete was conducted in accordance with a **modified version**¹² of ASTM C 633¹³. The standard tensile test is performed with a 2.54 cm diameter coated substrate which is epoxy bonded to a similar uncoated fixture (termed as the "pull-off bar"). In the present work the pull-off bar, 5.24 cm long x 2.54 cm diameter, was directly bonded to the zinc coating of the concrete. The pull-off bars were surface roughened **by grit** blasting prior to being smeared with a small amount of epoxy and attached, under moderate pressure of -2.1 kPa , to the zinc coated concrete. Any excess epoxy was wiped away from the base of the pull-off bar.

In several tests the samples displayed unusually high readings of bond strength which were attributed to the epoxy bonding directly to the concrete since it could penetrate the zinc coating. The locus of failure in such instances is not indicative of stresses that a coating may experience under service **conditions**.¹⁴ Therefore, in the above described instances, the epoxy adhesion strength to the concrete was **being** tested in preference to that of the coating. A film of **commercial** concrete sealer was used to fill the pores of the concrete to prevent such failures.

A test fixture **was** constructed to **accommodate** tensile testing of large specimens, Fig. 2. Two steel plates, 18 cm x 18 cm x 1.27 cm were connected by four circular rods, 15.24 cm long x 2.54 cm diameter. The bottom plate had a hole which was slightly larger than 2.54 cm. The coated substrate with the pull-off bar attached was placed on the bottom plate so that the pull-off bar protruded through the hole. The top and the bottom of the test apparatus (not indicated in Fig. 2 but attached to the hydraulic **Instron** tensometer) fitted into universal joints to allow for uniaxial alignment.

RESULTS AND DISCUSSION

The results of the adhesion strength and deposition efficiency (Figs. 3 to 5) can be viewed as topographical maps which show certain **surface** features. The **3-D** maps and contours extend beyond the test region and, therefore, this empirical modeling can under certain circumstances allow experimental extrapolation into untested **regions**.

Table 2 contains the coefficients of all the terms in Equation 1 for each of the 3-D graphs generated. The method of least squares **was** used in determining the coefficients for each of the terms. These **coefficients** define the curve and also indicate the dependence of each term on the value of the property; and, therefore, these coefficients establish the key **parameter(s)** which impact the bond strength and DE. For example, Fig. 3 examines DE at a gas pressure at 551 **kPa**. It is noticed by inspection of the contour plot that DE is more dependent on standoff distance than on **arc-current**. Increasing the standoff distance by 100% **from** 5 to 10 cm at 20 A arc current yields an absolute decrease in DE of 10%; **i.e., from** 57% to 47%. Conversely, the same magnitude increase in arc current does not produce an equivalent change in DE. Thus, on changing arc current from 20 A to 40 A, an increase of **100%**, at a standoff **distance** of 5 cm, leads to a DE change of approximately 1.5%. The DE is about 6.7 times more sensitive to change of standoff distance than to change in arc current.

Figure 3 also shows a "saddle point" located at ~ 40 to 80 A for a standoff of -12 to 18 cm. Such regions, although they may not encompass the highest DE parameters, are of practical interest since they infer that the process is quite tolerant to variations in these major thermal spray parameters.

Similar information can be obtained from Table 2. The coefficient for arc current, **b₁**, is 0.30 and the coefficient for standoff distance, **b₂**, is -9.01. This indicates that standoff distance has greater influence on DE than arc current. The sign of the coefficient indicates an increasing or decreasing dependence on property. For example, the negative sign for the standoff distance, indicates a negative dependence and infers that the DE decreases as the distance increases. A positive value of the coefficient indicates that the property of interest (DE) decreases **with** respect to an increasing parameter value (standoff distance).

An objective of performing these experiments **was** to establish the optimal parameter settings to **perform** thermal **spraying** on a large scale. The parameter set chosen should be optimized for both bond strength and DE. Often this is not possible since optimizing one set of parameters to yield favorable results for one property (**i.e.,** bond strength) may not produce favorable results for the other property (**i.e.,** DE). For example Fig. 4 shows bond strength variation with respect to standoff distance and gas pressure at an arc current of 45 amps. The X indicates the region in parameter space with the highest value of bond strength (1.86 **MPa**). The corresponding graph of DE, Fig. 5, is also marked with this X, and indicates a DE of **47%** which is **significantly** less than the 60% that is achievable. The experimental results indicate that a compromise can **be** achieved by decreasing the standoff distance by 2.54 cm to increase the DE **while** still maintaining a relatively high bond strength.

Low standoff distances lead to higher values of DE and this is attributed to the geometry of the spray pattern. The spray pattern has a wide divergence, so if the spray distance is close (5 cm), most of the material sprayed is incorporated into the coating. At longer spray distances, the large divergence is responsible for a **significant** velocity loss of droplets at the edge of the spray pattern or it takes too long for a droplet to reach the substrate. As a consequence, some droplets do not have **sufficient** dwell time in the flame to melt completely and others **resolidify** prior to reaching the substrate. Hence, the **semi**-molten droplets fall off, miss the target and become overspray or the solidified droplets bounce from the substrate surface.

An increase in gas pressure increases the bond strength due to higher velocities. The higher velocities cause spray particles to more likely form an appropriately flattened microstructure which enhances mechanical anchoring to the substrate. Increasing the arc current slightly increases the bond strength at low standoff distances. It also adds more **enthalpy** to the plasma, thus more energy is added to the spray droplets. The added enthalpy causes the droplets to become less viscous, thereby allowing greater penetration of the zinc into the porous concrete. This effect diminishes at larger standoff distances.

The goodness of fit test was used to validate the RSM model. The model is valid when the observed values of property and calculated values of property are close to each other. The Root Mean Square (RMS) of the differences between the observed and calculated values of property (**i.e.** bond strength) are presented in Table 3. The percentages indicate that the model accurately describes the observed values of property.

The values of bond **strength** cannot be compared directly with other published values due to variation in test conditions and equipment. These variations include concrete properties such as **mix** proportions, age, extent of **curing** and degree of carbonation; different surface preparation and use of testing apparatus with greater accuracy and control than field pull-off testers. The bond strengths of **1 to 2 MPa** reported in this work are of similar magnitude to those listed by **Howell¹⁵** and slightly lower than those obtained by **Brousseau et al.^{5,6}** It is not uncommon for the bond strengths of thermally sprayed materials to exhibit very high variability.^{**16,17**}

The parameter optimization method presented in this paper is also applicable to other thermal spray processes, such as twin wire arc and flame spraying, to different materials and to different measures of coating quality. For example, adhesion strength after a period of anode operation or a **microstructural** index such as coating porosity could be optimized in the same manner. Future work should examine the compatibility of adhesion strength and deposition efficiency with long-term anode performance to ensure that durability and **service** are maximized.

CONCLUDING REMARKS

Response Surface Methodology has been demonstrated to be an effective and efficient means to determine optimum thermal spray parameters for thermal sprayed zinc anodes on concrete. The dependence of tensile adhesion (bond) strength and deposition efficiency on standoff distance, arc current and gas pressure can be defined. The 3-D and 2-D presentations of data are intended to act as guides for the thermal sprayer to better understand the spray process. Such empirical modeling can be applied to many **infrastructural** processes that rely on optimization of processes.

The Single Wire Arc Plasma process is suitable for applying zinc to concrete. A short standoff distance (7 cm for the single wire system) is most useful for spraying large structures due to a reasonably high deposition efficiency (**>60%**) and adequate bond strength (**>2.07 MPa**). Neither the deposition efficiency nor the bond strength are strongly dependent on arc current and, therefore, a level of 35 A is sufficient since this is most cost effective. An increase in gas pressure leads to high bond strengths; and about 448 **kPa** is expected to be satisfactory from a practical viewpoint.

ACKNOWLEDGMENTS

The authors wish to thank The New York State Science and Technology Foundation, Flame Spray Industries, Inc., and Mr. Sang-Ha Leigh for support and assistance.

REFERENCES

1. R.A. **Carello**, D.M. Parks and J.A. Apostolos, "Development, Testing and Field **Application** of Metallized Cathodic Protection Coatings on Reinforced Concrete Substructures," California Department of Transportation, **Report No. FHWA/CA/TL-89/04**, May 1989.
2. J.A. Apostolos, D.M. Parks and R.A. **Carello**, "Cathodic Protection of Reinforced Concrete Using Metallized Zinc." *Materials Performance*, Vol. 26, No. 12, **1987**, 22-28.
3. R.J. Kessler, and R.G. Powers, "Zinc Metallizing for Galvanic Cathodic Protection of Steel Reinforced Concrete in a Marine Environment," **CORROSION/90**, Paper No. 324. (Houston, TX: NACE International, 1990).

4. D.G. Manning, "Cathodic Protection of Concrete Highway Bridges," in C.L. Page, K.W.J. **Treadaway**, and P.E. **Bamforth**, (Eds), Corrosion of Reinforcement in Concrete, Elsevier Science, Essex, 1990, 486-497.
5. R. Brousseau, M. **Arnott**, S. Dallaire and R. Feldman, "Factors Affecting Adhesion on Concrete of Arc-Sprayed Zinc," Corrosion, Vol. 48, No. 11, 1992, 947-952.
6. R. Brousseau, M. Arnott, and S. Dallaire, "The Adhesion of Metallized Zinc Coatings on Concrete- Part 1," **CORROSION/93**, Paper No. 331, (Houston, TX: NACE International, 1993).
7. Product Literature for Single Wire Arc Plasma, Flame Spray Industries, Stony Brook, New York.
8. T. **Troczyński** and M. **Plamondon**, "Response Surface Methodology for Optimization of Plasma Spraying," Journal of **Thermal Spray Technology**, Vol. 1. No. 4, 1992, 293-300.
9. **G.E.P**Box and N.R. Draper, Empirical Model Building and Response Surfaces, John Wiley and Sons, New York, 1987.
10. ASTM C 143-90, "Test Method fo Slump of Hydraulic Cement Concrete", Pub. ASTM, 1916 Race Steet. Philadelphia, PA 19103-1187, USA.
11. ASTM C 39-86, "Test Method for Compressive Strength of Cylindrical Concrete Specimens", Pub. ASTM, 1916 Race Steet, Philadelphia, PA 19103-1187, USA.
12. **S.H.Leigh** and **C.C.Berndt**, "A Test for Coating Adhesion on Flat Substrates", accepted for publication in J. Thermal Spray Technol., to be published Vol. 3, No. 3, 1994.
13. ASTM C 633-79, "Test Method for Adhesion or Cohesive Strength of Flame-Sprayed Coatings", Pub. ASTM. 1916 Race Steet, Philadelphia, PA 19103-1187, USA.
14. C.C. Berndt, "Instrumented Tensile Adhesion Tests on Plasma Sprayed Thermal Bamer Coatings", J. Mater. Eng., Vol. 11, 1989, 275-282.
15. K.M. Howell, "Evaluation of Bond Strength and Testing Equipment for Spray-Applied Coatings on Concrete Surfaces," **CORROSION/92**, Paper No. 198, (Houston, TX: NACE International, 1992).
16. P. **Ostojic** and C.C. **Berndt**, "The Variability in Strength of Thermally Sprayed Coatings", Surface and Coatings Technology, Vol. 34, 1988, 43-50.
17. C.C. Berndt and C.K. **Lin**, "Measurement of Adhesion for Thermally Sprayed Materials", J. Adhesion Sci. Technol., Vol. 7, No. 12, 1993, 1235-1264.

Table 1. Concrete Mix Proportions

MATERIAL	QUANTITY
Type I Cement	367 kg/m ³
Water	202 kg/m ³
Sand	918 kg/m ³
Coarse Aggregate	817 kg/m ³
NaCl	7.2 kg/m ³
Superplasticizer	10 ml/kg cement

Table 2. Constants for the coefficients expressed in Equation 1. The column titled "plot" indicates the variable that was held constant. a. Tensile strength, b. Deposition efficiency

a. Tensile strength

Plot	b ₀	b ₁	b ₂	b ₃	b ₄	b ₅
5 cm	-234.	-16.9	18.4	-0.0370	0.2430	-0.099
10 cm	-430	7.84	10.2	0.0004	-0.0811	-0.056
15 cm	-134	-6.68	12.0	-0.0100	-0.0864	-0.075
30 A	-230	8.59	25.9	-0.5520	-0.0332	1.500
45 A	-755	21.3	78.1	-0.0089	-0.3130	-10.30
60 A	-190	12.3	-36.4	-0.3500	-0.0631	5.590
448 kPa	150	1.50	-10.7	-0.6130	0.0226	4.160
551 kPa	164	2.60	-6.23	-0.3250	-0.0022	1.180
690 kPa	486	2.66	68.6	-0.3590	0.2280	-8.53

b. Deposition efficiency

Plot	b ₀	b ₁	b ₂	b ₃	b ₄	b ₅
5 cm	80.0	-0.84	0.11	0.0127	-0.0011	-0.005
10 cm	46.3	0.05	0.24	-0.0035	0.0028	-0.002
15 cm	37.4	0.07	0.32	-0.0021	0.0012	-0.002
30 A	116	-0.60	-13	0.0810	0.0003	0.466
45 A	40.5	0.92	-8.0	-0.0152	-0.0059	0.745
60 A	57.2	0.51	-6.8	-0.0293	-0.0033	0.709
448 kPa	96.8	-0.90	-8.8	0.0336	0.0083	0.494
551 kPa	68.2	0.30	-9.0	-0.0064	-0.0024	0.738
690 kPa	44.0	0.72	-4.2	-0.0940	-0.0030	0.688

Table 3. Goodness of fit values*. a. Tensile adhesion strength. b. Deposition efficiency

a. Tensile adhesion strength

Constant parameter	Average deviation from model (kPa)	Average deviation from model (%)	Average RMS deviation from model (kPa)	Average RMS deviation from model (%)
5 cm	110	7.7	44	3.4
10 cm	54	3.7	17	1.4
15 cm	70	5.9	29	2.5
30 A	46	3.2	17	1.2
45 A	110	8.5	42	3.3
60 A	620	4.1	24	1.6
448 kPa	35	5.1	14	1.1
551 kPa	110	7.0	44	2.8
690 kPa	112	7.8	44	3.4

* RMS = Root mean square

b. Deposition efficiency

Constant parameter	Average deviation from model (Y ₀)	Average deviation from model (%)	Average RMS deviation from model (Y ₀)	Average RMS deviation from model (%)
5 cm	0.9	1.6	0.4	0.6
10 cm	0.8	1.4	0.3	0.6
15 cm	0.2	0.4	0.1	0.2
30 A	0.9	1.7	0.3	0.7
45 A	0.5	0.9	0.2	0.4
60 A	0.9	1.6	0.4	0.7
448 kPa	0.7	1.4	0.3	0.5
551 kPa	0.4	0.8	0.2	0.3
690 kPa	1.3	2.6	0.5	1.0

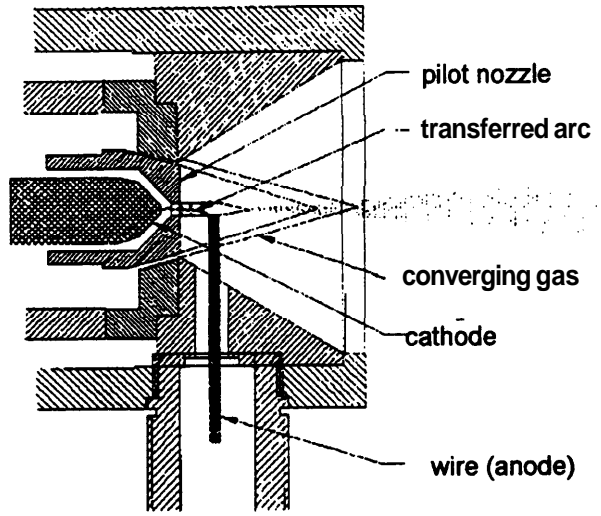


Figure 1. Schematic of the single wire arc plasma process.

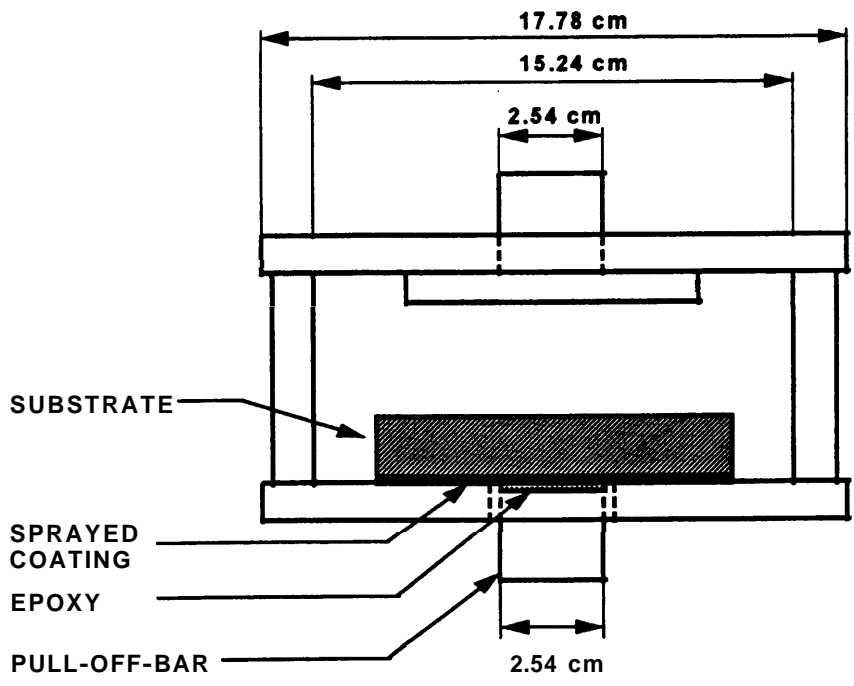
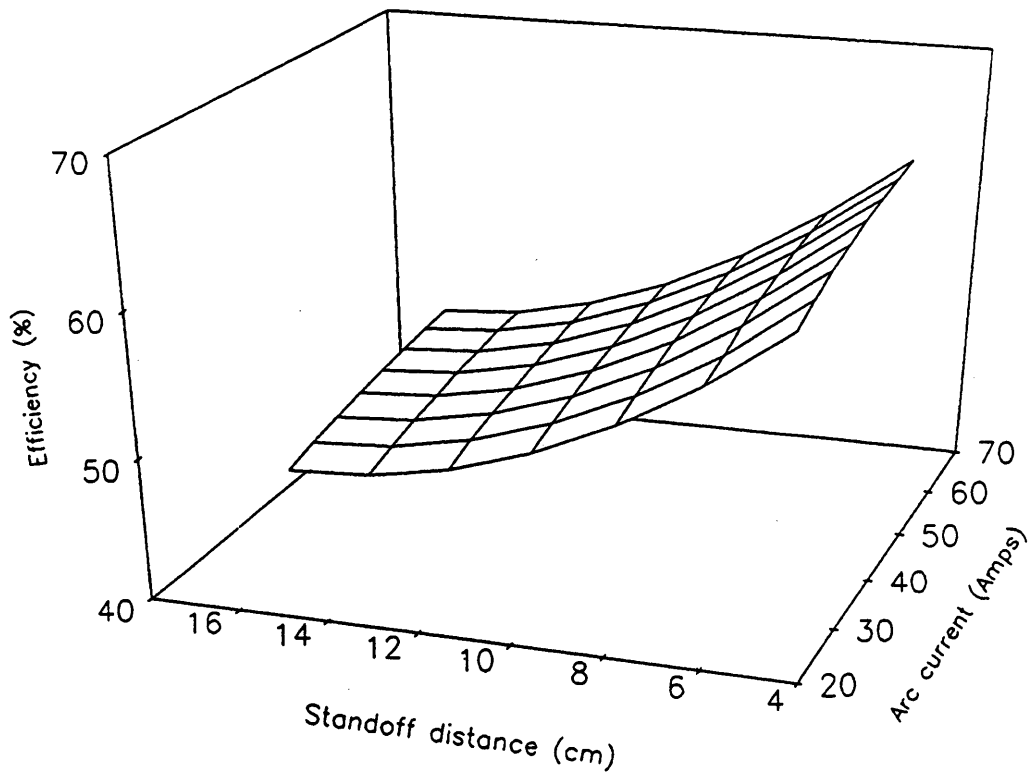
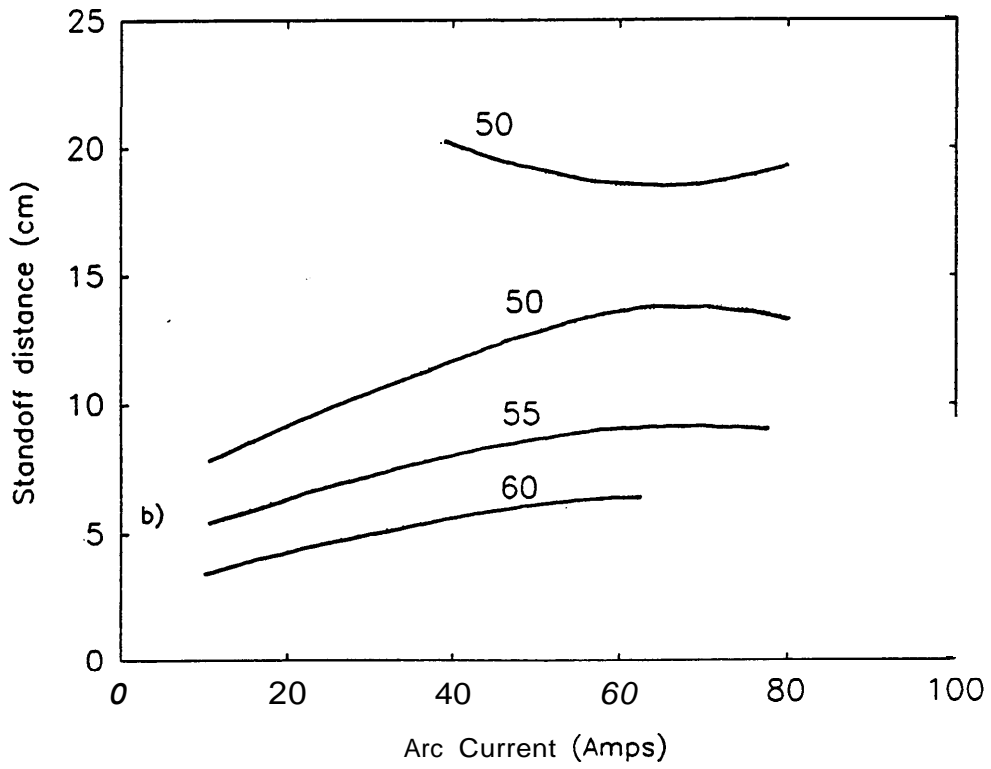


Figure 2. Adhesion strength test apparatus (side view)



a)



b)

Figure 3. Deposition efficiency at 551 kPa pressure. a. 3-D surface plot. b. Contour plots of constant deposition efficiency (in %).

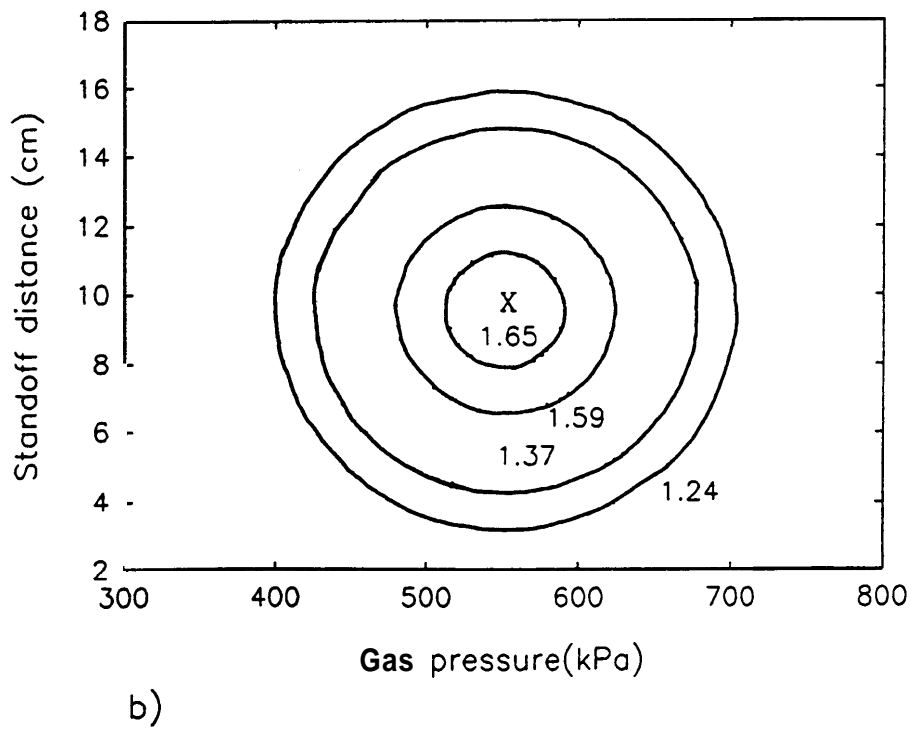
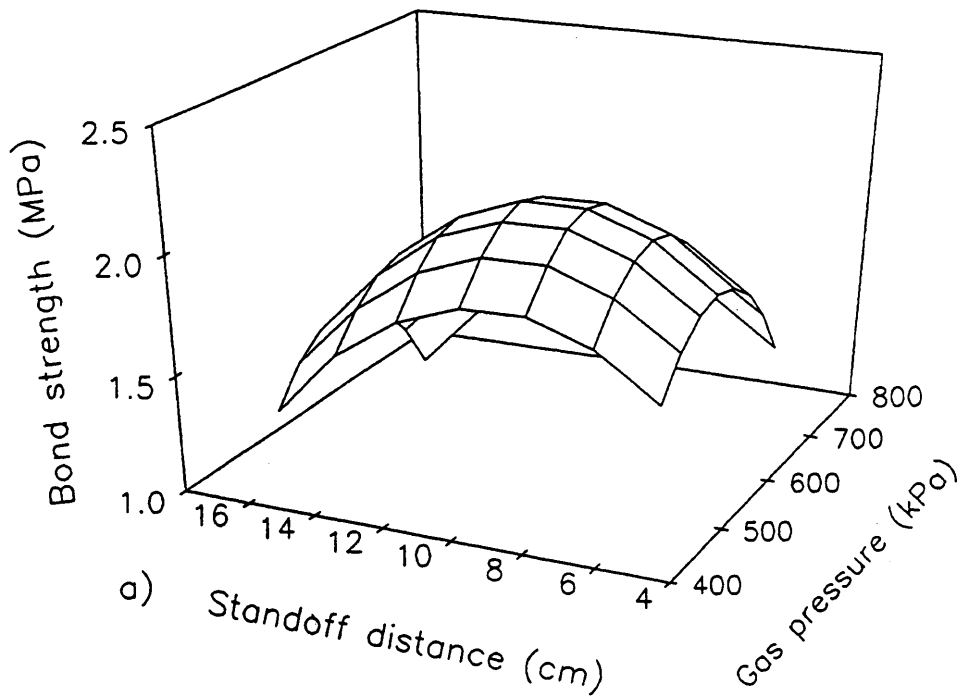


Figure 4. Bond strength at 45 amps arc current. a. 3-D surface plot. b. Contour plots of constant strength (in MPa) The X denotes the same set of spray parameters for the corresponding point shown in Fig. 5.

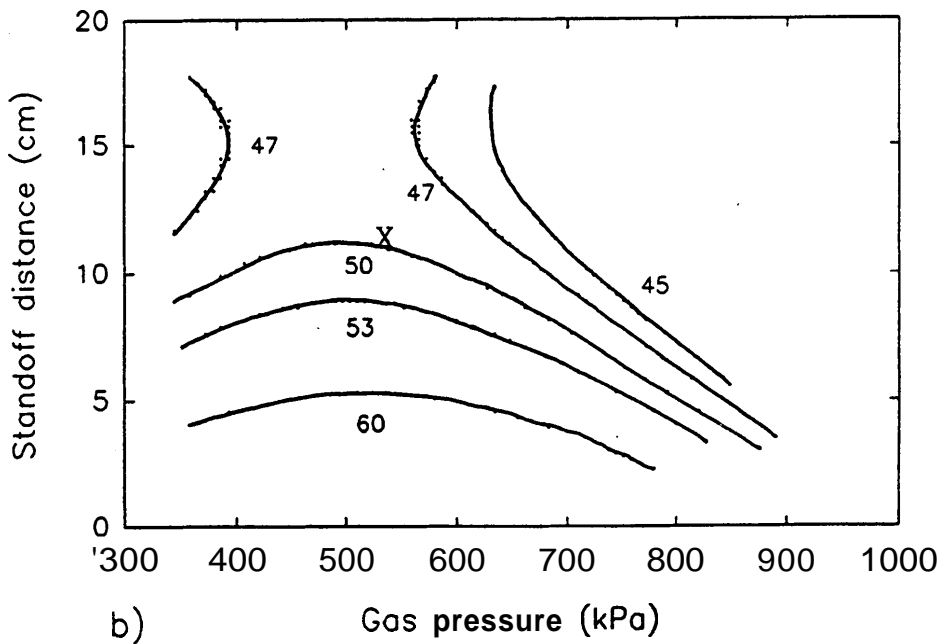
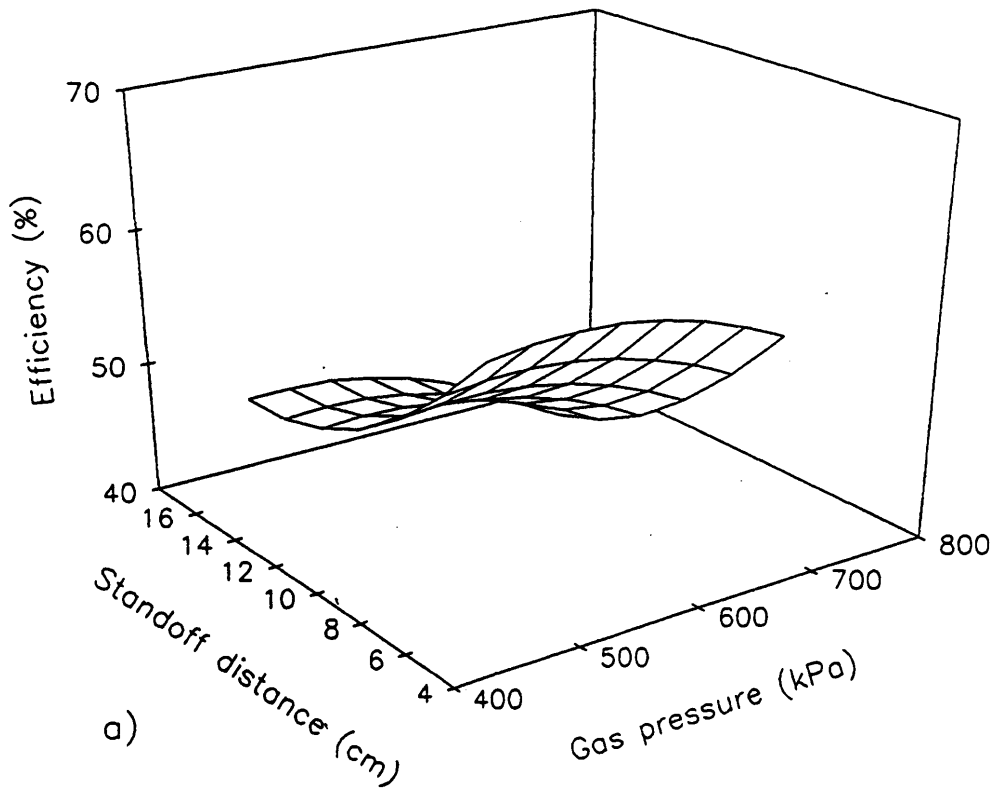


Figure 5. Deposition efficiency at 45 amps arc current. a. 3-D surface plot. b. Contour plots of constant deposition efficiency (in %). The X denotes the same set of spray parameters for the corresponding point shown in Fig. 4.